J. Plasma Phys. (2023), *vol*. 89, 895890104
Published by Cambridge University Press
doi:10.1017/S0022377822001015

Research on plasma vertical displacement calculation based on neural network

H.H. Song[1,2], **B. Shen**[1,†], **Q.P. Yuan**[1,†], **B.H. Guo**[3], **Y.H. Wang**[1], **D.L. Chen**[1], **R.R. Zhang**[1] **and B.J. Xiao**[1]

[1]Institute of Plasma Physics, Chinese Academy of Sciences, PO BOX 1126, Hefei 230031, PR China

[2]University of Science and Technology of China, Hefei 230031, PR China

[3]College of Physics and Optoelectronic Engineering, Shenzhen University, Shenzhen 518060, PR China

(Received 31 May 2022; revised 23 September 2022; accepted 23 September 2022)

Plasma vertical displacement control is essential for the stable operation of tokamak devices. The traditional plasma vertical displacement calculation method is not suitable for balancing speed and accuracy simultaneously, which is necessary for real-time feedback control. In this study, neural networks are used to rapidly detect vertical displacement recognition. Based on a fully connected neural network, the vertical displacement calculation model is trained and tested using magnetic data of approximately 2000 shots. To compare the effects of different inputs on vertical displacement calculation, different magnetic measurement diagnostic signals are used to train and test the model. Compared with a full magnetic measurement dataset, 39 magnetic measurement signals (38 magnetic probes and plasma current) show better accuracy with mean square error <0.0005. The model is tested using historical experimental data, and it demonstrates accurate vertical displacement calculation even in the case of a vertical displacement event. In general, neural network algorithm has great application potential in vertical displacement calculation.

Key words: neural network, tokamak, vertical displacement, magnetic measurement signals

1. Introduction

In contemporary tokamak devices, the method of plasma cross-section extension is typically used to improve the confinement performance of plasma for obtaining high-parameter plasma; this method is also applicable for future tokamak devices (Liu 2015). For the elongated plasma equilibrium configuration, there is a natural axisymmetric vertical instability, and it is one of the main reasons causing large disruption. Feedback control of plasma vertical instability is an effective method to achieve stable operation of tokamak plasma (Wang 2018). If the vertical displacement control can be detected more quickly and accurately, the adverse effect on discharge can be effectively reduced, and plasma with better performance can be obtained. To reduce the adverse effects of vertical instability, a four-channel digital signal processing controller is used in the TCV device in Switzerland for controlling

† Email addresses for correspondence: biaoshen@ipp.ac.cn, qpyuan@ipp.ac.cn

the vertical displacement of plasma at a frequency of 200 kHz. ASDEX-U in Germany is equipped with a passive feedback system, which significantly mitigates the growth rate of vertical displacement (Gruber, Lackner & Pautasso 1993). A passive plate is used in the vacuum chamber of the KSTAR device in Korea to increase the passive control ability of the device for ensuring vertical instability (Jhanga *et al.* 1999). At the JET, an extreme shape controller is used to enhance shape control during the transient phases of plasma current ramp-up and ramp-down; moreover, a current limit avoidance system is implemented to avoid saturation of the actuators with these transient phases (De Tommasi *et al.* 2014). NSTX-U, KSTAR and other similar devices have attempted to implement real-time methods for estimating the vertical displacement velocity using magnetic flux loops; based on the vertical displacement velocity, a good control effect has been obtained for these devices (Pomphrey, Jardin & Ward 1989; Ward & Hofmann 1994; Gates *et al.* 2006). In DIII-D, a neural network is used to receive the equilibrium data from RTEFIT for estimating the vertical displacement growth rate, and then proportional–integral–differential control is used for adjusting the plasma configuration in the plasma control system (PCS) (Sammuli, Barr & Humphreys 2021).

Plasma vertical displacement cannot be measured directly; the plasma equilibrium reconstruction code EFIT (Huang 2017) uses external diagnostic measurement data to reconstruct the actual plasma configurations and solve the Grad–Shafranov equation in the vacuum region. Plasma shape control parameters including vertical displacement are provided; however, the EFIT calculation cycle is at the millisecond level, which cannot meet the requirements of vertical displacement fast control. The vertical displacement control system on EAST is used under the condition of a certain equilibrium; based on the rigid model RZIP, a matrix is deduced to estimate the vertical displacement (Yuan *et al.* 2013). The PCS (Qiping 2009) calculates the corresponding control command; then, it transmits the command to a fast control power supply, and finally, the power supply realises the control. The EAST device in China has fast vertical displacement control with a 100 μs control cycle (Liu 2015; Huihui & Qiping 2020). When the actual plasma configuration is greatly different from the assumed equilibrium configuration, the vertical displacement estimated by the matrix deviates, resulting in an unsatisfactory control effect. In recent years, with rapid advances in neural networks, increasing numbers of researchers have realised that neural network tools may provide unique advantages in research on controlled fusion. On HL-2A, a hybrid neural network model based on bidirection long short-term memory network and long short-term memory network is used for plasma position prediction, resulting in excellent prediction (Yang *et al.* 2020). In this study, neural networks are used to explore the advantages of vertical displacement control.

Neural networks are used to fit the vertical displacement, remove the restrictions of simplified physical models, establish a new mapping relationship between electromagnetic measurement signals and vertical displacement, and provide a new calculation method for vertical displacement. To calculate the vertical displacement using a neural network, a vertical displacement database is first established; thereafter, an appropriate neural network model is chosen for training and testing after analysing the test results.

The rest of this paper comprises four parts. Section 2 describes the composition and processing of the database according to the research steps. The principle and structural parameters of the neural networks are introduced in § 3. The test results of the models are introduced, and the advantages and disadvantages of different models are compared in § 4. Finally, a brief conclusion is presented in § 5.

https://doi.org/10.1017/S0022377822001015 Published online by Cambridge University Press

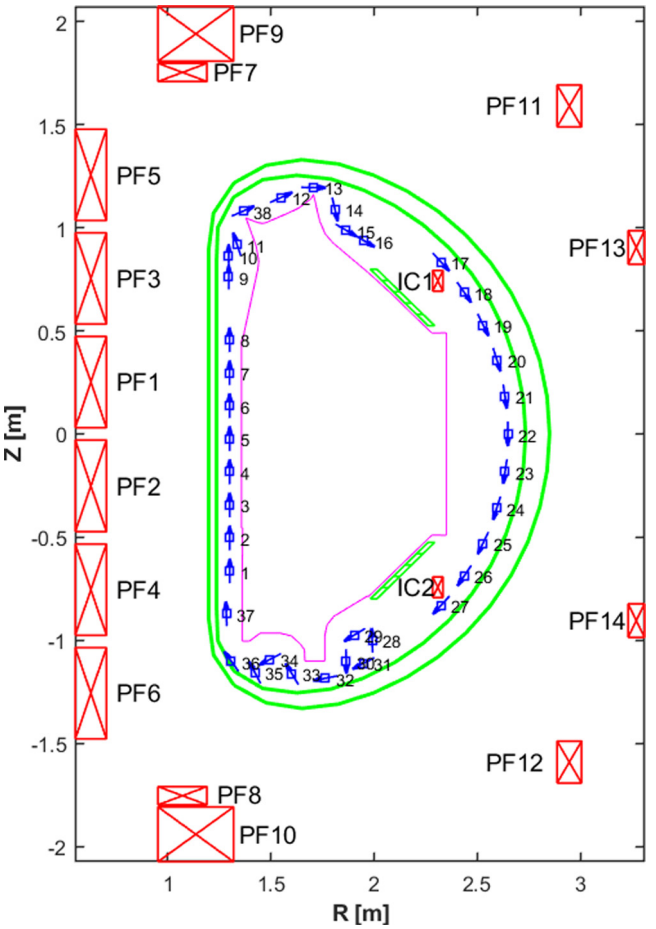

FIGURE 1. EAST device interface diagram.

2. Database construction

At EAST, the centre of gravity of the current is different in all standard divertor configurations, including double null, upper single null and lower single null (Yuan *et al.* 2013). To ensure model accuracy, the database should contain sufficient sample data for all the different configurations. Further, one single shot on EAST contains several diagnosis signals (Guo, Chen & Shen 2021; Guo, Shen & Chen 2021). Of these, only 88 vertical displacement control signals are chosen, containing 14 poloidal field (PF) coil current signals, 35 magnetic flux (FL) loops, 38 magnetic probes and plasma current. These signals are closely related to the vertical displacement. The EAST device interface diagram and cross-section of probe position are shown in figure 1.

The vertical displacement calculated using EFIT is selected as the target of the network model; 2000 shots covering EAST shot numbers from 97 500 to 99 500 in the MDSplus database are analysed. The time scale and sampling rate of signal data collected by PCS are different from those of EFIT. Therefore, all data were first aligned chronologically. The signals collected by PCS were re-sampled according to the time axis of EFIT. Second, different collected signals represent different physical meanings, and the order of magnitude of data is not the same, and it requires standardised data processing.

https://doi.org/10.1017/S0022377822001015 Published online by Cambridge University Press

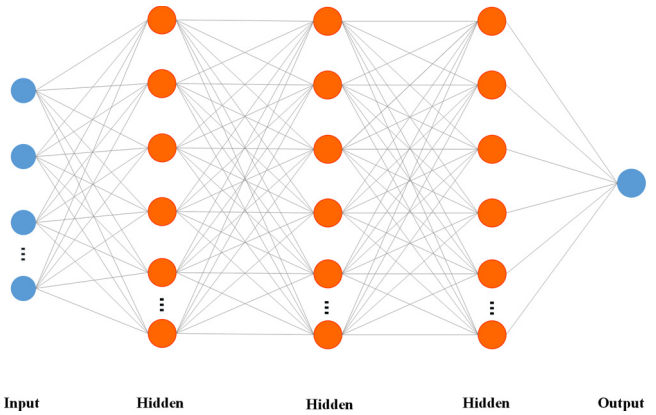

FIGURE 2. Fully connected neural network architecture.

Typical standardisation methods include Z-score standardisation, logistic standardisation and maximum–minimum values standardisation. Z-score standardisation is applicable for situations where the maximum and minimum values of unknown data and the sample distribution are very discrete, and the logistic standardised sample index data are relatively concentrated on both sides of 0. Considering the actual demand, the normalisation method of maximum and minimum values can arrange all data chronologically between [0, 1]. Numerical problems caused by orders-of-magnitude differences are avoided. The data were then shuffled and divided into training and test sets.

To explore the influence of different magnetic measurement signals on vertical displacement, input data in the database are divided into two groups after data processing. In one group, all magnetic measurement signals are used as the input data of training, and in the other group, magnetic probe signals are selected as the input data of training. The output data are all vertical displacement values calculated by EFIT. For these two sets of data, models are established for training.

3. Construction of neural network

A fully connected neural network is one of the most widely used neural network models. It comprises three parts, namely an input layer, a hidden layer and an output layer (Hu & Zeng 2009). The input layer of the fully connected neural network is equivalent to the stimulus given by the outside world, and it is considered as the input data. The hidden layer is the equivalent of the human brain where neurons interact. The output layer represents the response of neurons after multi-level interaction. The fully connected neural network contains multiple neurons and transmits signals forward and errors back through neurons, and thus it has the advantages of self-organisation, self-adaptability and self-learning, and it can deal with complex problems quickly and stably. Its structure is shown in figure 2.

The model structure of the neural network is determined using experimental results. It comprises five layers. The input layer comprises 128 neurons, and three hidden layers are set with 16 neurons in each layer. The number of nodes in the hidden layer is set according to the formula $n_1 = \sqrt{n+m}+a$ (Shen, Wang & Gao 2008), where n is the number of neurons in the input layer, m is the number of neurons in the output layer and a is a constant between [1, 10]. The structure is shown in table 1.

https://doi.org/10.1017/S0022377822001015 Published online by Cambridge University Press

Layer name	Number of cells	Activation function	Number of parameters
Input layer dense	128	Relu	5120
Hidden layer dense	16	Relu	2064
Hidden layer dense	16	Relu	272
Hidden layer dense	16	Relu	272
Output layer dense	2	Sigmoid	34

TABLE 1. Structural parameters of neural network.

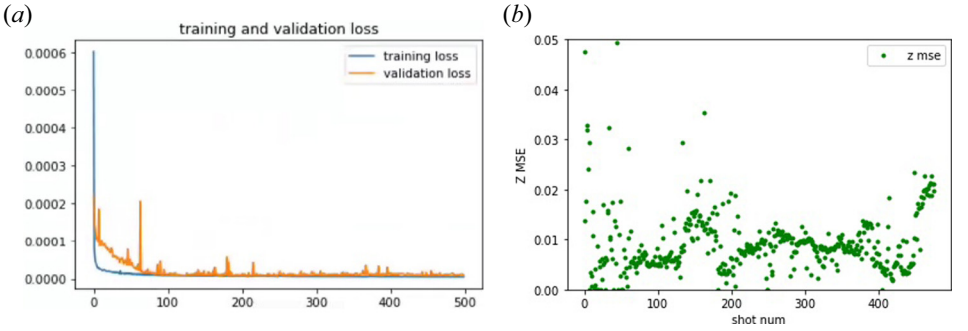

FIGURE 3. The 88-input model training and test loss function diagram (*a*) and mean square error (MSE) of test set (*b*).

4. Model training and testing

4.1. *All magnetic measurement signals model*

All electromagnetic measurement signals (total number = 88) are used as input to train the model, and it is labelled as the 88-input model. According to neural network training rules, we train the model 500 times. The loss function of training and testing is shown in figure 3(*a*); the horizontal axis shows the training iterations, the blue line represents the training loss function value and the orange line represents the test loss function value. By constantly adjusting the model parameters, the loss is minimised and the model reaches the optimal convergence state, in which the maximum error of the model training results is 0.003186. Then, 500 shots with different configurations whose shot number is from 99 501 to 100 000 were used as the test. The mean square error of the model-predicted value of each test shot is shown in figure 3(*b*); the horizontal axis is the number of shots, and each point represents the mean square error between the model-predicted value and the target value of the shot data. The mean square error for the test data is concentrated between [0.00, 0.02].

The test set contains all configurations, and one configuration shot @100000 is selected for testing (figure 4). The horizontal axis in figure 4 is time (seconds) and the vertical axis is vertical displacement (metres). The red line is the vertical displacement result calculated by EFIT and the blue line is the vertical displacement result fitted by the neural network model. The mean square error is 0.000002.

4.2. *Model of magnetic probe signals*

Only magnetic probe signals and plasma current signal are used as input to train the model in the second group; the PF coil current and FL loops are discarded. The model

https://doi.org/10.1017/S0022377822001015 Published online by Cambridge University Press

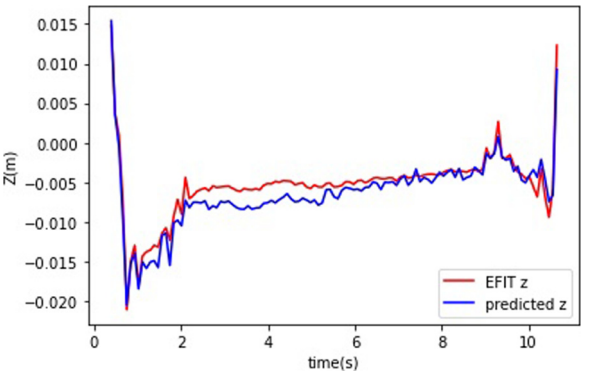

FIGURE 4. The 88-input model fitting vertical displacement result diagram @100000.

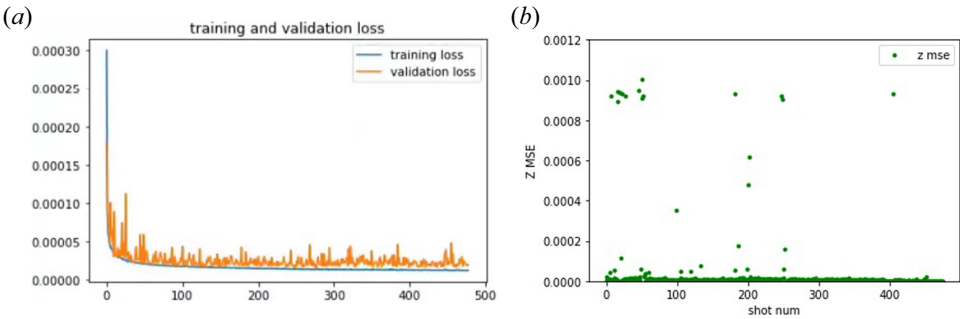

FIGURE 5. The 39-input model training and test loss function diagram (*a*) and mean square error (MSE) of test set (*b*).

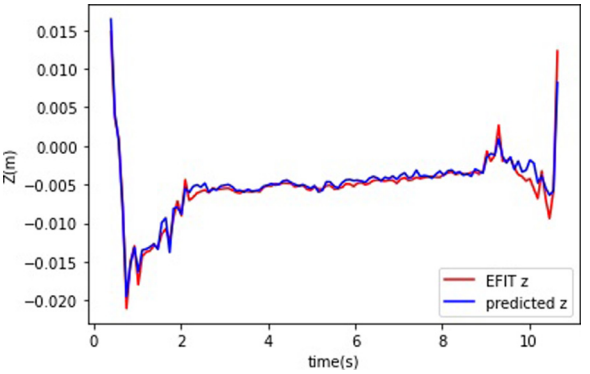

FIGURE 6. The 39-input model fitting vertical displacement result diagram @100000.

of magnetic probe signals is labelled as the 39-input model. The test results are shown in figure 5. The model training and test loss function values are $\leq$0.00005, and the mean square errors for test data are concentrated between [0.0000, 0.0005].

Similar to § 4.1, one configuration shot @100000 is selected for testing (figure 6). The mean square error is 0.000001.

https://doi.org/10.1017/S0022377822001015 Published online by Cambridge University Press

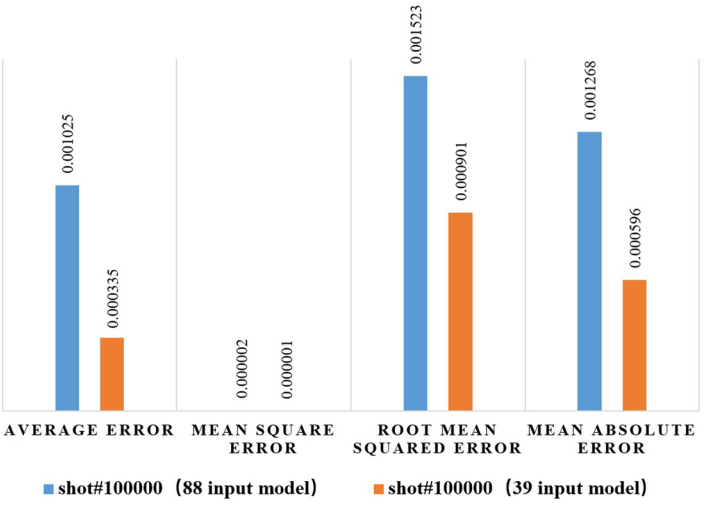

FIGURE 7. Error parameter values of the two models @100000.

4.3. *Comparison of the two models*

The models with 39 and 88 inputs are compared; the mean square errors of the same test set data are smaller and more concentrated. The relevant error parameters of configuration are shown in figure 7.

As shown in figure 7, for the test shot @100000, all error parameter values of the 39-input model are less than those of the 88-input model. Compared with the 39-input model, the 88-input model added PF coil current signals and FL signals as inputs. For PF coil current signals, the PF coils are located outside a vacuum vessel, which is considered as a passive structure. The PF coil current changes, especially high-frequency changes, are shielded by the vacuum vessel, implying that the PF coil current cannot directly reflect the plasma vertical position at the current moment. The FL signals are integral signals, which are mainly contributed by the ohmic field. The effects of plasma vertical displacement on the FL signals are approximately 0.05 mV mm^{-1} (for 400 kA plasma), and they are easily affected by electronic noise. At the same time, fewer input signals greatly improve the speed of model calculation. The 39-input model is chosen for application in this study.

Specific configuration experimental shot @102913 whose vertical displacement changes drastically, that is, the shot disrupted due to a vertical displacement event, is selected for testing the 39-input model; the test results are shown in figure 8. Same as in figure 4, the red line is the vertical displacement result calculated by EFIT and the blue line is the vertical displacement result fitted by the neural network model. The maximum error between them is 0.007494, the mean square error is 0.000004 and the mean absolute error is 0.001520. Compared with shot@100000, error parameters are slightly larger, but are much less than the maximum controllable error of vertical displacement. Thus, the proposed model could also achieve effective control in a particular configuration.

5. Conclusion

This study is based on the magnetic probe measurement data of the EAST tokamak device and the vertical displacement data calculated by EFIT. The relationship between magnetic measurement signals and vertical displacement is explored using neural networks, and the better model is tested for accuracy. By simulating neural network

https://doi.org/10.1017/S0022377822001015 Published online by Cambridge University Press

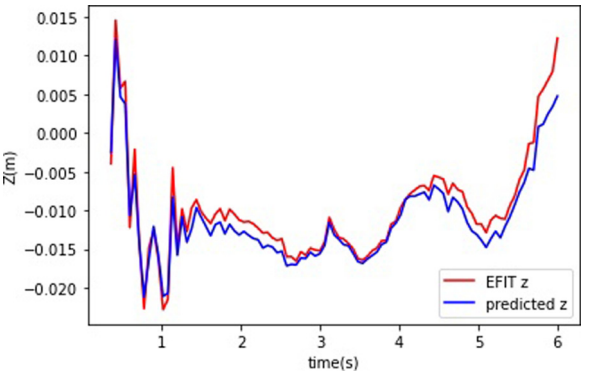

FIGURE 8. The 39-input model fitting vertical displacement result diagram @102913.

tests, better control of vertical displacement in the future and the prediction of vertical displacement is achieved. Fewer signals are required to estimate the vertical displacement, realising faster control of vertical displacement. The next step of this study is to make the model a real-time one and carry out experimental verification of the vertical displacement control system.

Acknowledgements

Editor William Dorland thanks the referees for their advice in evaluating this article.

Funding

This work is supported by the National MCF Energy R&D Program of China (no. 2018YFE0302100) and the National Natural Science Foundation of China (no. 11905250, no. 12075285).

Declaration of interests

The authors report no conflict of interest.

REFERENCES

DE TOMMASI, G., *et al.* 2014 Shape control with the XSC during plasma current ramp-up and ramp-down at the JET tokamak. *J. Fusion Energy* **33**, 149–157.

GATES, D.A., KESSEL, C., MENARD, J., *et al.* 2006 Progress towards steady state on NSTX. *Nucl. Fusion* **46** (3), 22–28.

GRUBER, O., LACKNER, K. & PAUTASSO, G. 1993 Vertical displacement events and halo currents. *Plasma Phys. Control. Fusion* **35B**, 191.

GUO, B.H., CHEN, D.L. & SHEN, B. 2021 Disruption prediction on EAST tokamak using a deep learning algorithm. *Plasma Phys. Control. Fusion* **63**, 115007.

GUO, B.H., SHEN, B. & CHEN, D.L. 2021 Disruption prediction using a full convolutional neural network on EAST. *Plasma Phys. Control. Fusion* **63** (2), 025008.

HU, J. & ZENG, X. 2009 An efficient activation function for BP neural network. In 2009 *International Workshop on Intelligent Systems and Applications*, pp. 1–4. IEEE.

HUANG, Y. 2017 Study of MHD equilibrium reconstruction and plasma control based on GPU parallel computation. PhD thesis, University of Chinese Academy of Science.

HUIHUI, S. & QIPING, Y. 2020 Design and implementation of fast control on the vertical displacement based on high-speed acquisition. *J. Instrum. Technol*. **4**, 37–42.

https://doi.org/10.1017/S0022377822001015 Published online by Cambridge University Press

JHANGA, H., KESSELB, C., POMPHREY, N., JARDIN, S.C., LEE, G.S. & CHANG, C.S. 1999 Design calculations for fast plasma position control in Korea superconducting tokamak advanced research. *Fusion Engng Des*. **45**, 101–115.

LIU, L. 2015 The simulation and experimental study of passive stability and active control for EAST vertical instability. PhD thesis, University of Chinese Academy of Science.

POMPHREY, N., JARDIN, S.C. & WARD, D.J. 1989 Feedback stabilization of the axisymmetric instability of a deformable tokamak plasma. *Nucl. Fusion* **29** (3), 465.

QIPING, Y. 2009 Plasma control system with Linux cluster structure. PhD thesis, University of Chinese Academy of Sciences.

SAMMULI, B.S., BARR, J.L. & HUMPHREYS, D.A. 2021 Avoidance of vertical displacement events in DIII-D using a neural network growth rate estimator. *Fusion Engng Des*. **169**, 112492.

SHEN, H.-Y., WANG, Z. & GAO, C. 2008 Determining the number of BP neural network hidden layer units. *Tianjin Univ. Technol*. **5**, 13–15.

WANG, Y. 2018 EAST shape and position control opentimization and system identification. PhD thesis, University of Chinese Academy of Science.

WARD, D.J. & HOFMANN, F. 1994 Active feedback stabilization of axisymmetric modes in highly elongated tokamak plasmas. *Nucl. Fusion* **34** (3), 401–415.

YANG, B., LIU, Z., SONG, X. & LI, X. 2020 Design of HL-2A plasma position predictive model based on deep learning. *Plasma Phys. Control. Fusion* **62**, 125022.

YUAN, Q., XIAO, B., LUO, Z., *et al.* 2013 Plasma current, position and shape feedback control on EAST. *Nucl. Fusion* **53** (4), 043009.

https://doi.org/10.1017/S0022377822001015 Published online by Cambridge University Press